

ОБЪЕДИНЕННЫЙ
ИНСТИТУТ
ЯДЕРНЫХ
ИССЛЕДОВАНИЙ
ДУБНА

E7-85-64

M.T.Magda*, A.Pop*, A.Săndulescu

**PROJECTILE BREAKUP
AND CLUSTER EMISSION
IN HEAVY ION REACTIONS
AT LOW ENERGY**

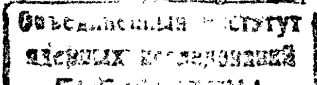
Submitted to "ЯФ"

* Institute for Physics
and Nuclear Engineering, Bucharest, Romania

1985

I. INTRODUCTION

Previous work in the heavy ion physics devoted to particle emission, was concentrated on two extreme cases: light particle emission (p, d, α -particles)^{/1,2/} and heavy particle emission (close to the mass of the projectile or fission fragments). A special case represents the emission of α particles, as it was shown in the pioneer work of Britt and Quinton^{/3/}. In recent time an increased interest was manifested for the emission of intermediate mass particles with $2 \leq Z \leq 17$ ^{/4-11/}. The existing experimental data show that even particles with $Z > 2$ have quite large emission cross sections and strongly peaked forward angular distributions. On the other side, the energy distributions are continuous and have an evaporation-like shape with an angle-dependent temperature. We remark that the highest energy in the particle spectra is close to the one given by the kinematics of a two-body process^{/5/}. The maxima in the energy distributions are around the energy corresponding to the projectile velocity and their widths are larger than expected for an evaporation spectrum. Another feature of the intermediate Z particle emission is the strong dependence of the cross section on the particle type: the Z-dependence of the cross sections is not monotonous but has an oscillatory behaviour which follows the values of the separation energy of the projectile into two fragments^{/4/}. We also notice that in many cases the energy distributions present two components: the experimentally decreasing evaporation component and a flat, monotonous one, suggesting a direct process as the projectile breakup, for example. It was recently shown that projectile breakup expected to occur at higher than 10 MeV/nucleon energies was also present in the reactions at lower energies^{/9,12-17/}. The aim of this work is to determine the contribution of the breakup process to the emission of intermediate mass particles. Of course, the reaction mechanism is more complicated and other processes, as statistical or preequilibrium emission, are not excluded^{/18/}. But in case of particles more complex than α -particles, their emission at low energies by compound nucleus evaporation is questionable unless their existence (preformation) in the nucleus is accepted. From this point of view, the breakup of the projectile is a process favoring the emission of complex particles. We concentrated on the measurements performed in Dubna^{/5-8/} for small emission angles, particularly for 0° .



Such experimental data are the only ones which exist so far and provide the best experimental information to put into evidence the breakup process.

II. STATISTICAL EMISSION OF CLUSTERS FROM THE COMPOUND NUCLEUS

In the first stage of this work we estimated the emission cross sections predicted by the statistical model and compared them with the experimental ones. A simple, and of course approximate variant of the statistical model was used which determines the total emission cross section. Then the emission of a particle ν with the energy ϵ_ν , $\epsilon_\nu + d\epsilon_\nu$ is written as^{/19/}:

$$\sigma_\nu d\epsilon_\nu \sim (2s_\nu + 1)\mu_\nu \sigma_\nu \epsilon_\nu \rho(E^* - E_{\text{rot}}(J) - B_\nu - \epsilon_\nu) d\epsilon_\nu, \quad (1)$$

where μ_ν , s_ν , B_ν are the mass, spin and binding energy of the particle ν , and σ_ν is the inverse reaction cross section. As usually in the statistical model, ρ represents the level density of the residual nucleus, having an excitation energy equal to E and a rotational energy E_{rot} corresponding to the J angular momentum:

$$\rho(E, J) \sim (2J + 1)E^{-\frac{1}{2}} \exp 2\sqrt{aE}. \quad (2)$$

The E^* excitation energy of the compound nucleus was expressed by the relation $E^* = E_{\text{in}}^{\text{c.m.}} + Q - \langle E_{\text{rot}} \rangle$, where $E_{\text{in}}^{\text{c.m.}}$ is the bombarding energy in the c.m. and Q - the formation energy of the compound nucleus. The average rotational energy of the compound nucleus $\langle E_{\text{rot}} \rangle$ corresponds to the average value of its angular momentum obtained by using the transmission coefficients (T_l) as weighting factors. The transmission coefficients were calculated in the parabolic model of Thomas^{/20/}. For the sake of simplicity, the ratios σ_ν/σ_α as obtained from eq.(1) were calculated for a particle ν and the α -particle, for the energy corresponding to the maximum of the evaporation distribution: $\epsilon_\nu = V_\nu + T$. The Coulomb barrier is given by the expression

$$V_\nu = \frac{(Z - Z_\nu)Z_\nu}{R}, \quad (3)$$

where Z and Z_ν are the atomic numbers of the compound nucleus and the particle ν , respectively. The interaction radius R was defined as $R = 1.5[(A_{\text{CN} - \nu})^{1/3} + A_\nu^{1/3}]$ for all particles, except the proton in case of which $R = 1.5(A_{\text{CN}} - 1)^{1/3}$. The nuclear temperature $T = \sqrt{E/a}$ was obtained by a method of iteration; the level density parameter $a = (A_{\text{CN} - \nu})/8$.

The inverse reaction cross sections were calculated in the sharp cut-off classical approximation:

$$\sigma_\nu(\epsilon_\nu) = \pi R_{\text{ACN} - \nu}^2 (1 - V_\nu/\epsilon_\nu). \quad (4)$$

We remark that the ratio of the cross sections obtained by this procedure represents upper limits because it was assumed that all the emitted clusters do exist in the nucleus, therefore have been performed.

We considered so far that all involved nuclei are spherical. It is well known that due to the high angular momenta brought into the compound nucleus by the projectile, the compound nucleus is strongly deformed what leads to a lowering of the barriers for particle emission. Then an amplified emission of the heavier particles like Li, Be, C is expected as it was shown by Blann and Komoto^{/21/}. We took this fact into account by using in calculations lower values of the barriers. The lowering factors for the barriers were estimated from Blann's paper^{/21/} as shown in the Table.

This method for estimating the statistical emission cross sections was checked for the experimental data of Xenoulis et al.^{/22/}.

A typical result is represented by the continuous lines in Fig.1 for the case of the $^{181}\text{Ta} + ^{22}\text{Ne}$ (178 MeV) system^{/5/}. The dotted lines represent another variant of the statistical model, in which the fact that various particles are emitted from different regions of the $E^* - J$ plane is taken into account^{/23/}. For estimating the influence of this effect on the cross sections, we consider that the emission of particles with $2 \leq Z \leq 4$ occurs from a region of high excitation energy and lower angular momenta of the compound nucleus. Therefore the corresponding rotational energy of the compound nucleus is smaller than the average rotational energy determined by the above-mentioned method. This leads to larger values of the cross sections as one can see in Fig.1. A comparison of the ratios σ_ν/σ_α with the experimental values shows that in case of the H isotopes the theoretical predictions are close to the experiment showing that the contribution of the statistical emission is important. The experimental data of the other isotopes are lying higher than the theoretical ones suggesting that their emission proceeds by other mechanisms (direct mechanism). We remark that the experimental values of the σ_ν/σ_α ratios could be lowered in an artificial manner, because α -particle emission is strongly amplified in heavy ion reactions due to the contribution of various processes. Turning back to Fig.1 we notice a dramatic increase of the difference between theory and experiment in the case of ^8He . It is obvious that the statistical emission of exotic, neutron rich, isotopes like

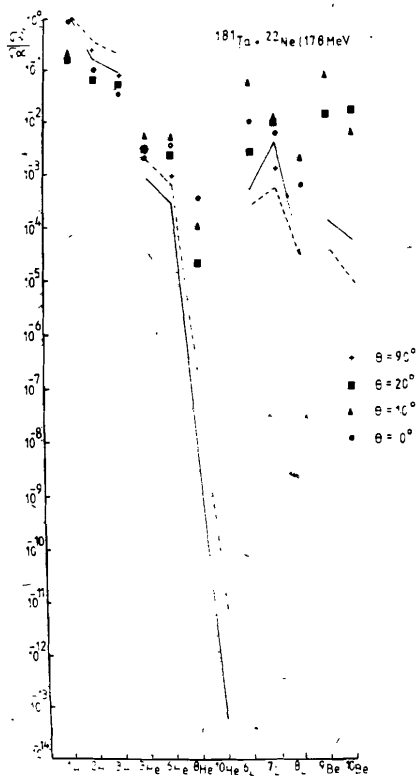


Fig.1. The experimental values of the maximum of the energy distributions and the related values predicted by the statistical model.

Table

| Particle type (isotope) | |
|----------------------------|------|
| H | 0.97 |
| He | 0.84 |
| Li | 0.86 |
| Be | 0.85 |
| B | 0.82 |

^8He and ^{10}He occurs with negligibly small cross sections, while in case of ^3He and ^6He the statistical contribution is not excluded. Similar results were obtained for other systems presented in papers ^{/5-7/}.

III. PROJECTILE FRAGMENTATION AND CLUSTER EMISSION

The angular and energy distributions of the particles emitted by the projectile breakup were calculated in the frame of the model elaborated earlier by Serber ^{/24/} and recently developed by other authors ^{/13,25,26/}.

We consider the process $m_P + m_T \rightarrow m_{F_1} + m_{F_2} + m_T$ where P , T , F_1 and F_2 mean the projectile, target and respectively the fragments simultaneously emitted after the projectile broke up in the field of the target nucleus. Then a two-body or a three-body process is possible. In case of a two-body process, the unobserved fragment fuses with the target nucleus; such reac-

tions are called incomplete fusion reactions ^{/27/}. In the three-body process the observed fragment as well as the unobserved fragment and the target nucleus are assumed in the final state.

Starting from the momentum distribution of the observed fragments, determined by the coupling of the momentum due to the incident motion of the projectile to its intrinsic momentum relative to the other fragment in the projectile

$$\bar{P}_{F_1} = \frac{m_{F_1}}{m_P} \bar{P} + \bar{P} \quad (5)$$

one obtains the square of the transition matrix element:

$$|T|^2 \sim \frac{1}{\pi^2} \frac{(2\mu E_s)^{1/2}}{[2\mu E_s + (\frac{m_{F_1}}{m_P} \bar{P} - \bar{P}_{F_1})^2]^2} \quad (6)$$

Here μ represents the reduced mass; and E_s , the separation energy of the projectile into two fragments.

Then the cross section in the three-body case is written

$$\frac{d^2 \sigma}{d\Omega_1 dE_{F_1}} \sim \frac{1}{\pi^2} m_{F_1} (2\mu E_s)^{1/2} P_{F_1} \cdot S_{F_1} \times \int d\bar{P}_{F_2} d\bar{P}_T \frac{\delta(\bar{P}_{F_1} + \bar{P}_{F_2} + \bar{P}_T - \bar{P}) \delta(E_{F_1} + E_{F_2} + E_T + E_s - E_P)}{[2\mu E_s + (\frac{m_{F_1}}{m_P} \bar{P} - \bar{P}_{F_1})^2]^2} \quad (7)$$

The cross section for the two-body process is given by the following expression:

$$\frac{d^2 \sigma}{d\Omega_1 dE_{F_1}} \sim \frac{4}{\pi} m_{F_1} m_{F_2} P_{F_1} P_{F_2} \frac{\sigma_F S_F (2\mu E_s)^{1/2}}{[2\mu E_s + (\frac{m_{F_1}}{m_P} \bar{P} - \bar{P}_{F_1})^2]^2} \quad (8)$$

where the fusion cross section σ_F is determined by the fusion barrier between the unobserved fragment and the target nucleus according to an expression similar to (4).

The spectroscopic factor S_F ^{/28/} expresses the probability to find together the Z_{F_2} protons and N_{F_2} neutrons which have to be removed from the projectile to produce the observed fragment. According to Friedman ^{/28/} the spectroscopic factor is given by the following relation:

$$S_F = S_F(Z_{F_2}, N_{F_2}) / \sum_{N_{F_2} + Z_{F_2} = A_{F_2}} S_F(Z_{F_2}, N_{F_2}) \quad (9)$$

where A_{F_2} is equal to the number of particles extracted from the projectile. The function $S_F(Z_{F_2}, N_{F_2})$ is defined as follows:

$$S_F(Z_{F_2}, N_{F_2}) = \frac{Z_P! N_P!}{Z_{F_1}! N_{F_1}! Z_{F_2}! N_{F_2}!} \quad (9a)$$

We have introduced the spectroscopic factor in the existing formulation of the Serber model^{13,25,26/} in order to get the absolute values of the production cross sections for various isotopes. In this way a unique normalization factor is obtained by comparing the theoretical to the experimental cross section for one of the most stable observed fragments.

The corrections due to the projectile deceleration and fragment acceleration in the Coulomb field were introduced in the local momentum approximation. The asymptotic momenta were replaced with the effective "local" ones at the point where the fragmentation occurs:

$$\bar{P}_P^L = (1 - E_{C_1}/E_P)^{1/2} \bar{P}_P, \quad (10a)$$

$$\bar{P}_{F_1}^L = (1 - E_{C_2}/E_{F_1})^{1/2} \bar{P}_{F_1}, \quad (10b)$$

Here E_{C_1} and E_{C_2} represent the Coulomb energy of the projectile and the observed fragment respectively, calculated at the touching radius, where the breakup is supposed to occur due to both the nuclear and Coulomb interactions.

Both variants of the breakup model were employed by using the code SERBR^{29/}. The reaction energies and the separation energies of the particles from the projectile were determined with the existing tables^{30/}. Before comparing the theory with the experiment, the energy distributions were multiplied by the Fermi function $F(E, E_0) = 1/\{\exp[(E - E_0)/\delta E] + 1\}$ which takes into account the cut of the spectra in the region of low energies determined by the thickness of the ΔE detector. E_0 is the cutoff-energy; and δE , the energy resolution.

The analysis of some systems studied in Dubna^{5-8/} was performed with the above described procedure. The most complete experimental information was obtained for the $^{181}\text{Ta} + ^{22}\text{Ne}$ system: energy distributions of the H-, He-, Li- and Be-isotopes, were measured at $\theta_{\text{lab}} = 20^\circ$ and 141 and 178 MeV incident energies. For the last energy measurements have been also performed for the angles of 0, 10, and 90° . The energy distributions of He-isotopes emitted by the $^{181}\text{Ta} + ^{22}\text{Ne}$ system (178 MeV, $\theta_{\text{lab}} = 0^\circ$ and 10°) are represented in Fig.2. They

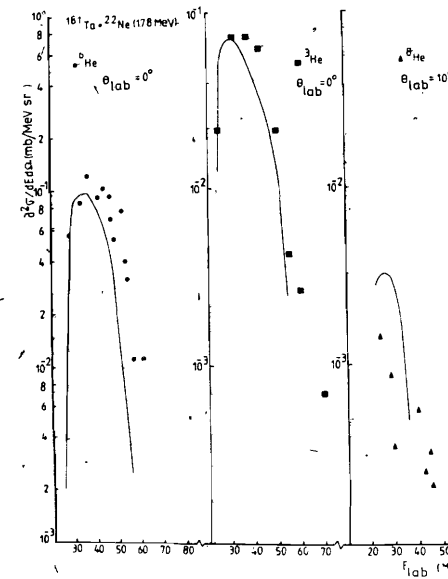


Fig.2. Experimental and theoretical energy distributions of the He-isotopes emitted in the $^{181}\text{Ta} + ^{22}\text{Ne}$ (178 MeV) reaction.

were calculated with the two-body variant of the Serber model in the assumption of a two-step (sequential) process: in a first stage of the reaction the projectile is excited and subsequently decays in the field of the target nucleus. The hypothesis of the two-step mechanism of the breakup process is supported by the existing correlation measurements intended to identify the mechanism of the projectile breakup in reactions at energies lower than 10 MeV/nucleon^{31/}. For describing the two-step character of the breakup process, an effective bombarding energy was calculated by subtracting from the kinetic energy of the projectile the excitation energy of an excited state of ^{22}Ne lying above the separation energy of the α particle ($E = 10.62$ MeV). It is interesting to mention that it was not necessary to change the value of the excitation energy according to the different separation energies of various isotopes. This shows that when the interaction between the projectile and the target takes place, a fraction of its kinetic energy is transformed into excitation energy, producing its deformation and subsequent fragmentation. We remark that in the case of the He-isotopes, as well as of the other isotopes (Li, Be), the three-body variant of the Serber model leads to a wider than experimental energy distribution. The distance where the breakup occurs is considered to be equal to the touching radius. As the system of the unobserved fragment and target nucleus is expected to be strongly deformed, the fusion barrier is lowered. This fact was accounted for in calculations by using a large parameter for the barrier radius, $r_0 = 1.45$ fm.

As one sees in Fig.2, the two-body variant of the Serber model describes well the spectra of the He-isotopes. A good agreement of the theory with the experiment is also obtained for the Li and Be-isotopes (Figs.3 and 4). We stress again the fact that a single normalization factor was used for a given projectile-target system, what proves the consistence of the theoretical analysis.

The angular distribution for ${}^7\text{Li}$ is shown in Fig.4 along with the theoretical one (the continuous lines) which describe well the width and maximum of the energy distributions for the three angles of detection (0° , 10° , and 20°) with a single normalization factor. In the case of the spectrum at 0° a tentative separation of the three-body breakup was done (dotted line in Fig.4). However, as obtained for the other fragments, the two-body breakup has the main contribution in the emission cross section. A special situation is observed in case of ${}^7\text{Li}$ spectrum at 90° , the shape and narrow width of which are rather evaporation like. Moreover, its amplitude is smaller than expected from the Serber model, what indicates that the evaporation component is more important at large angles.

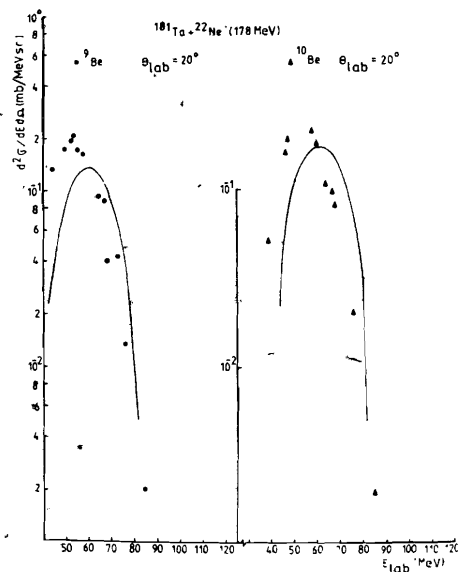


Fig.3. Experimental and theoretical energy distributions of the Be-isotopes emitted in the ${}^{181}\text{Ta} + {}^{22}\text{Ne}$ (178 MeV) reaction.

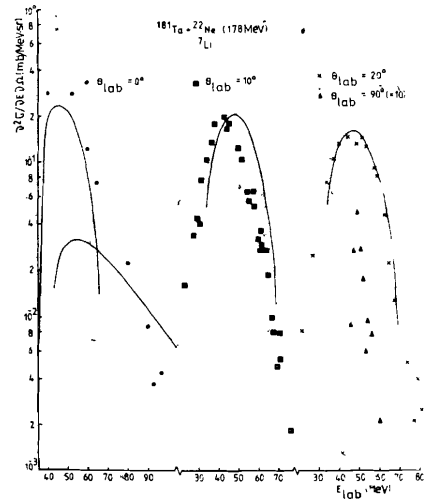


Fig.4. The angular and energy distributions of the ${}^7\text{Li}$ isotope emitted in the reaction ${}^{181}\text{Ta} + {}^{22}\text{Ne}$ (178 MeV).

The situation is different for the same system at the low energy of 141 MeV as shown in Fig.5. The two-body breakup (incomplete fusion) is no more possible because the energy of the unobserved fragment is lower than the fusion barrier between it and the target nucleus. The measured spectra are satisfactorily explained by the three-body process, as shown in Fig.5 for ${}^6\text{He}$, ${}^7\text{Li}$, and ${}^9\text{Be}$. This time again, the two-step character of the reaction was taken into account. The continuous and dotted lines (Fig.5) show the results for projectile excitations at

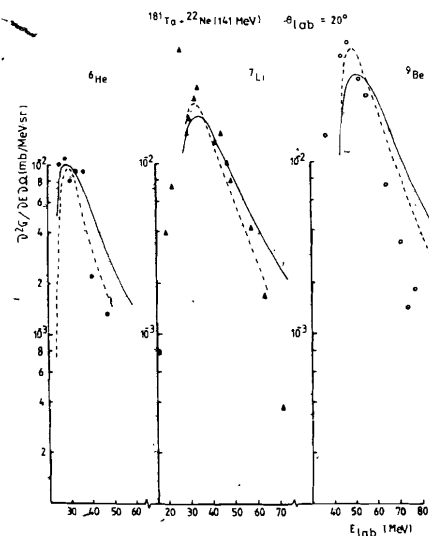


Fig.5. Experimental and theoretical energy distributions for the ${}^6\text{He}$, ${}^7\text{Li}$, and ${}^9\text{Be}$ isotopes emitted in the ${}^{181}\text{Ta} + {}^{22}\text{Ne}$ (141 MeV) reaction.

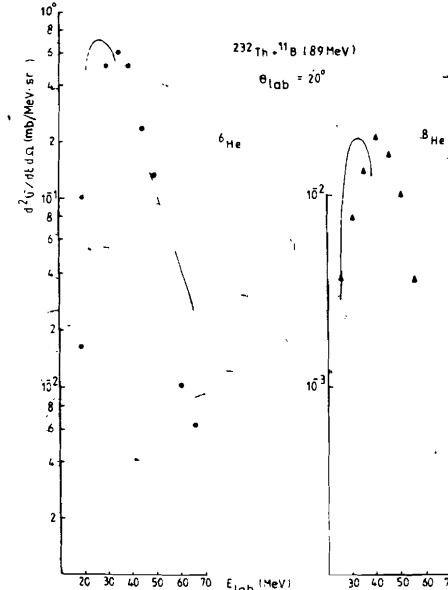


Fig.7. Experimental and theoretical energy distributions of ${}^6\text{He}$ and ${}^8\text{He}$ isotopes emitted in the ${}^{232}\text{Th} + {}^{11}\text{B}$ (89 MeV) reaction.

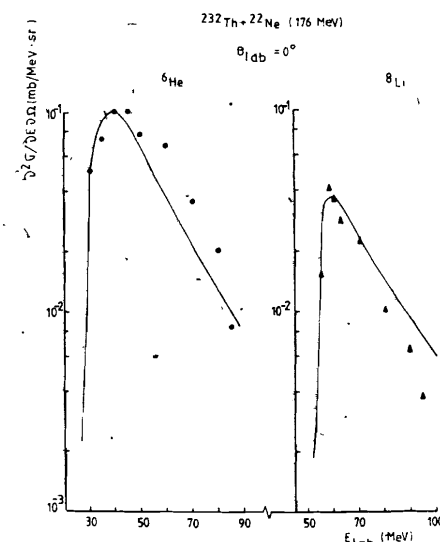


Fig.6. Experimental and theoretical energy distributions of the ${}^6\text{He}$ and ${}^8\text{Li}$ isotopes emitted in the ${}^{232}\text{Th} + {}^{22}\text{Ne}$ (178 MeV) reaction.

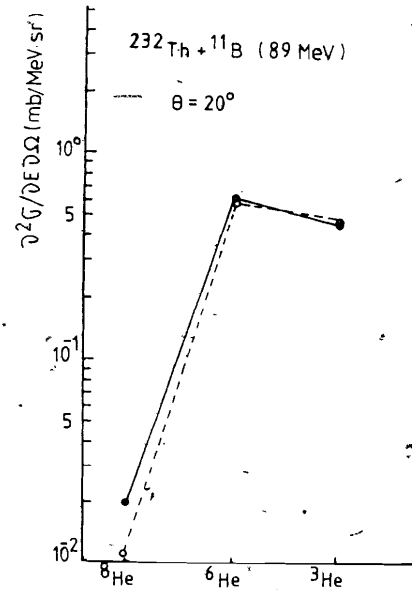


Fig.8. The comparison of the theoretical and experimental cross sections for He-isotope production in the ${}^{232}\text{Th} + {}^{11}\text{B}$ reaction.

The angular distribution for ${}^7\text{Li}$ is shown in Fig.4 along with the theoretical one (the continuous lines) which describe well the width and maximum of the energy distributions for the three angles of detection (0° , 10° , and 20°) with a single normalization factor. In the case of the spectrum at 0° a tentative separation of the three-body breakup was done (dotted line in Fig.4). However, as obtained for the other fragments, the two-body breakup has the main contribution in the emission cross section. A special situation is observed in case of ${}^7\text{Li}$ spectrum at 90° , the shape and narrow width of which are rather evaporation like. Moreover, its amplitude is smaller than expected from the Serber model, what indicates that the evaporation component is more important at large angles.

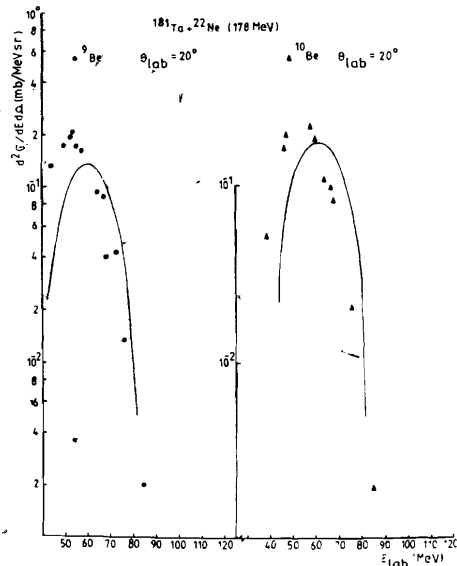


Fig.3. Experimental and theoretical energy distributions of the Be-isotopes emitted in the ${}^{181}\text{Ta} + {}^{22}\text{Ne}$ (178 MeV) reaction.

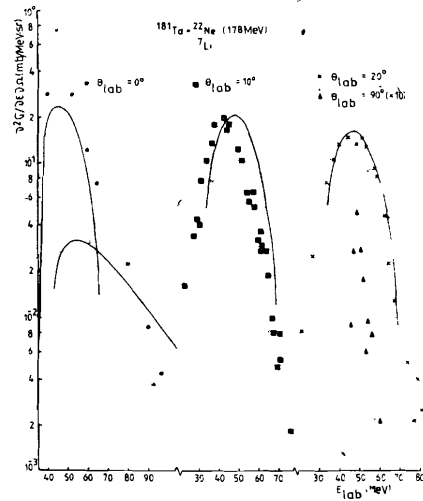


Fig.4. The angular and energy distributions of the ${}^7\text{Li}$ isotope emitted in the reaction ${}^{181}\text{Ta} + {}^{22}\text{Ne}$ (178 MeV).

The situation is different for the same system at the low energy of 141 MeV as shown in Fig.5. The two-body breakup (incomplete fusion) is no more possible because the energy of the unobserved fragment is lower than the fusion barrier between it and the target nucleus. The measured spectra are satisfactorily explained by the three-body process, as shown in Fig.5 for ${}^6\text{He}$, ${}^7\text{Li}$, and ${}^9\text{Be}$. This time again, the two-step character of the reaction was taken into account. The continuous and dotted lines (Fig.5) show the results for projectile excitations at

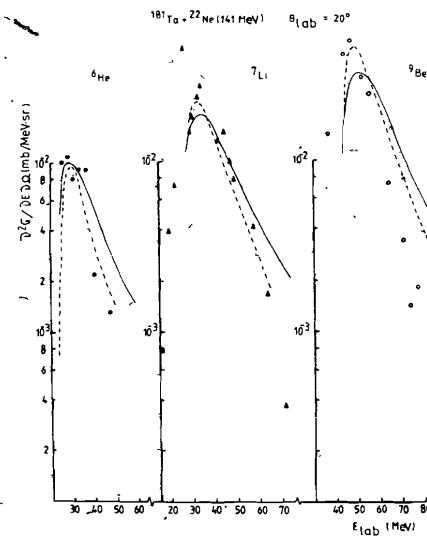


Fig.5. Experimental and theoretical energy distributions for the ${}^6\text{He}$, ${}^7\text{Li}$, and ${}^9\text{Be}$ isotopes emitted in the ${}^{181}\text{Ta} + {}^{22}\text{Ne}$ (141 MeV) reaction.

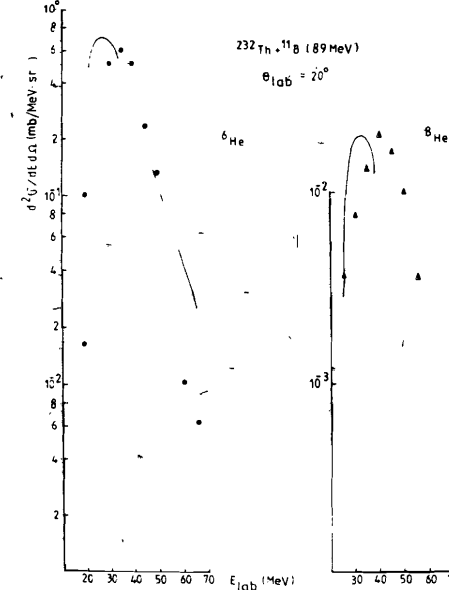


Fig.7. Experimental and theoretical energy distributions of ${}^6\text{He}$ and ${}^8\text{He}$ isotopes emitted in the ${}^{232}\text{Th} + {}^{11}\text{B}$ (89 MeV) reaction.

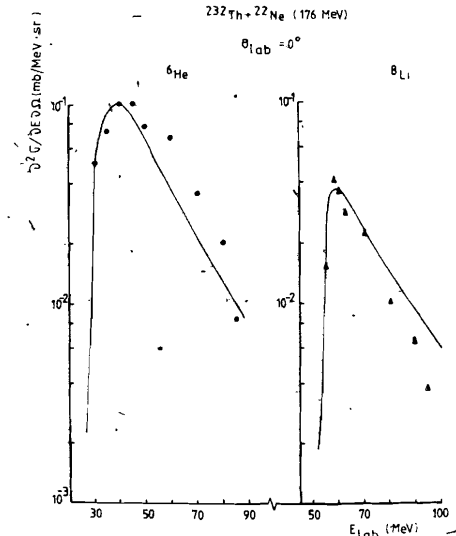


Fig.6. Experimental and theoretical energy distributions of the ${}^6\text{He}$ and ${}^8\text{Li}$ isotopes emitted in the ${}^{232}\text{Th} + {}^{22}\text{Ne}$ (178 MeV) reaction.

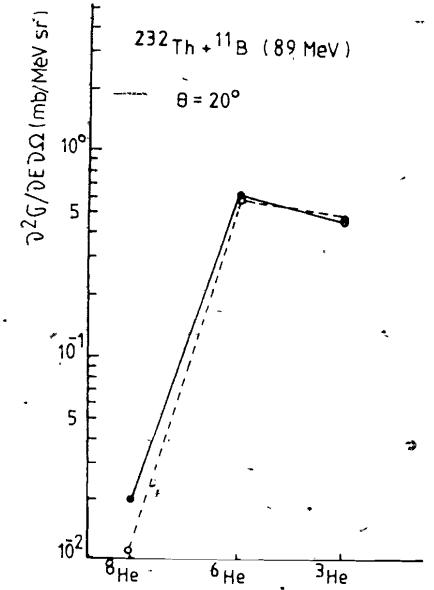


Fig.8. The comparison of the theoretical and experimental cross sections for He-isotope production in the ${}^{232}\text{Th} + {}^{11}\text{B}$ reaction.

10.62 and 15 MeV, respectively, in the first stage of the reaction.

The breakup process must be more dependent on the projectile than on the target nucleus. A comparison of both the studied systems $^{181}\text{Ta} + ^{22}\text{Ne}$ and $^{232}\text{Th} + ^{22}\text{Ne}$ reveals interesting in this context. Spectra obtained for some isotopes emitted in the $^{232}\text{Th} + ^{22}\text{Ne}$ reaction are shown in Fig. 6. As mentioned above, a unique value of the normalization factor was used. The interaction barrier being higher for this system, the two-body breakup has no contribution to the emission cross section which is entirely due to a three-body process.

We also analysed the data obtained for the $^{232}\text{Th} + ^{11}\text{B}$ which was intended to lead to the production of rare isotopes like ^{10}He [6,7]. The measured spectrum of ^6He is well explained by the Serber model (Fig. 7). The model doesn't work in the case of ^8He because the formation of a many-body final state: $^{11}\text{B} \rightarrow ^8\text{He} + 3\text{p}$. The phase-space factors in the present Serber calculations correspond only to the two- and three-body final state. On the other side, if the mechanism of the complex particle emission is the breakup of the projectile, it is not surprising that the ^{10}He isotope could not be obtained by the $^{232}\text{Th} + ^{11}\text{B}$ reaction, because the projectile has not enough neutrons to produce such a neutron-rich fragment.

In the context of exotic nuclei production it would be useful to predict the cross sections for ^{10}He production in case of various systems studied in Dubna. We showed in the analysis of experimental data that a unique normalization factor was determined for all the isotopes allowing to estimate the absolute values of the cross sections. Figures 8-10 show the experimental values of the cross sections at the maximum of the measured energy distribution (black points) and the theoretical predictions of the breakup model (open points). The agreement between theory and experiment is quite good, within a factor of two or three. However, a systematic tendency of overevaluation seems to manifest, presumably due to a second fragmentation of the weakly bounded particles, as for ex. ^6He , ^8He , ^{10}He , ^6Li , and ^8Li . Then the cross sections estimated for unstable particles have to be taken as upper limits.

IV. CONCLUDING REMARKS

The present analysis of the experimental information obtained in Dubna on the emission of clusters with $2 \leq Z \leq 4$ at lower than 10 MeV/nucleon energies shows that the breakup of the projectile is the main mechanism of their production. The experimental data have been analysed with the Serber model which was modified to describe the two-step character of the

breakup at these energies and to estimate the absolute values of the cross sections. The analysis of the experimental data shows that the breakup occurs in two steps and that the contribution of the two-body breakup (incomplete fusion) increases with the bombarding energy. It is interesting to remark that even from the only inclusive data available one can extract some information concerning the reaction mechanism by means of a detailed analysis.

We consider that projectile breakup occurring in these reactions is analogous to cluster (C, Ne) emission from the ground state of nuclei following their cold fragmentation [32]. A study of the potential energy of the system would give an insight on the forces determining its evolution as a three-body process and also the fusion of the unobserved fragment with the target nucleus.

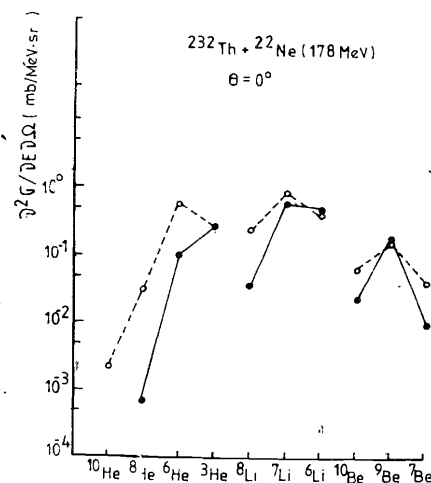


Fig. 9. The comparison of the theoretical and experimental cross sections for He-, Li-, and Be-isotope production in the $^{232}\text{Th} + ^{22}\text{Ne}$ reaction.

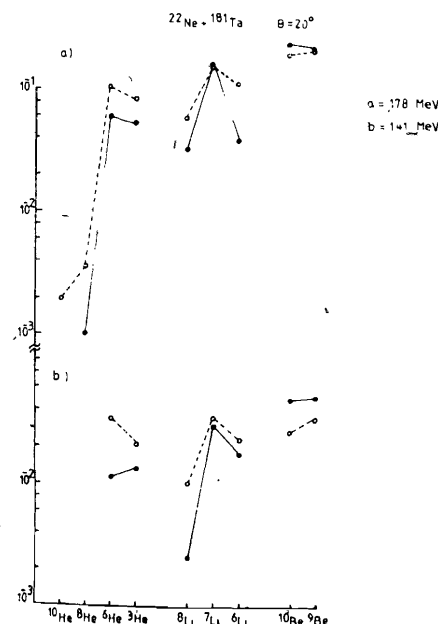


Fig. 10. The comparison of the theoretical and experimental cross sections for He-, Li-, and Be-isotope production in the $^{181}\text{Ta} + ^{22}\text{Ne}$ reaction.

The estimation of the production cross sections of various isotopes for some reactions which have been used to produce ^{10}He explains the negative result obtained so far by the small cross sections of such unstable nuclei.

The authors express their gratitude to Prof. Yu.Ts.Oganessian, Drs. V.V.Volkov, Yu.E.Penionzhkevich, C.Borcea and R.Kalpakchieva for useful discussions and suggestions. One of them (M.T.M.) thanks JINR for the possibility of working in the Laboratory of Nuclear Reactions, where much of this work has been done.

REFERENCES

1. Oganessian Yu.Ts. Proc. of the Int. School on Nucl. Struct. JINR, D4-80-385, Dubna, 1980, p.261.
2. Běták E., Toneev V.D. Sov.Journ.Part.Nucl., 1981, vol.12, p.1432.
3. Britt H.C., Quinton A.R. Phys.Rev., 1961, vol.124, p.877.
4. Volkov V.V. Izv.AN SSSR, 1981, vol.45, p.1810.
5. Borcea C. et al. Nucl.Phys., 1982, vol.A391, p.520.
6. Oganessian Yu.Ts. et al. Pisma v JETP, 1982, vol.36, p.104.
7. Oganessian Yu.Ts. et al. Izv. AN SSSR, 1982, vol.46, p.2218.
8. Borcea C. et al. Nucl.Phys., 1984, vol.A415, p.169.
9. Mateja F., Garman A. Phys.Rev.C, 1983, vol.28, p.1579.
10. Vaz L.C. et al. Zeit.f.Phys., 1983, A311, p.89.
11. Sobotka L.G. et al. Phys.Rev.Lett., 1983, vol.51, p.2187; 1984, vol.53, p. 2004.
12. Tabor S.L. et al. Phys.Rev.C, 1981, vol.24, p.960.
13. Tabor S.L., Dennis L.C., Abdo K. Phys.Rev.C, 1981, vol.24, p.2552.
14. Hugi M. et al. Nucl.Phys., 1981, A368, p.173.
15. Pop A. et al. Rev.Roum.Phys., 1984, vol.29, p.87.
16. Pop A. et al. IPNE Preprint, Bucharest, 1984.
17. Utsunomiya H. et al. Phys.Rev.C, 1984, vol.28, p.1975.
18. Běták E., Toneev V.D. JINR, E4-82-1983, Dubna, 1984.
19. Plasil F., Blann M. Phys.Rev.C, 1975, vol.11, p.508.
20. Thomas T. Phys.Rev., 1959, vol.116, p.703.
21. Blann M., Komoto T.T. Phys.Rev.C, 1981, vol.24, p.426.
22. Xenoulis A.C. et al. Phys.Lett., 1981, vol.106B, p.461.
23. Delagrangé H., Fleury A., Alexander J.M. Phys.Rev.C, 1977, vol.16, p.706.
24. Serber D. Phys.Rev., 1947, vol.72, p.1008.
25. Wu J.R. et al. Phys.Rev.C, 1979, vol.20, p.1284.
26. Matsuoka N. et al. Nucl.Phys., 1978, vol.A311, p.173.
27. Siwek-Wilczynska K. et al. Nucl.Phys., 1979, vol.A330, p.150.
28. Friedman W.A. Phys.Rev.C, 1983, vol.27, p.569.
29. Pop A. Ann.Rep. of the Heavy Ion Department, Bucharest, 1982-83.
30. Atomic Data and Nuclear Data Tables, 1976, vol.17.
31. Legrain R. Nucl.Phys., 1982, vol.A387, p.219c.
32. Săndulescu A., Poenaru D.N., Greiner W. Sov.Journ.Part. Nucl., 1980, vol.11, No.6, p.528.

Received by Publishing Department
on January 30, 1985.

Магда М.Т., Поп А., Сăндулеску А.

E7-85-64

Развал иона-снаряда и эмиссия кластеров с $2 \leq Z \leq 4$
в реакциях с тяжелыми ионами при низких энергиях

Экспериментальные данные, полученные в Дубне для эмиссии частиц с $2 \leq Z \leq 4$, проанализированы в рамках модели Сербера, измененной для того, чтобы описать двухступенчатый характер реакции развала и оценить абсолютные величины сечений образования разных изотопов. Было показано, что развал иона-снаряда является главным механизмом эмиссии кластеров промежуточной массы. Оцененные сечения образования ^{10}He обсуждаются в контексте его нестабильности.

Работа выполнена в Лаборатории ядерных реакций ОИЯИ.

Препринт Объединенного института ядерных исследований. Дубна 1985

Magda M.T., Pop A., Săndulescu A.

E7-85-64

Projectile Breakup and Cluster Emission
in Heavy Ion Reactions

Experimental data obtained in Dubna for the emission of particles with $2 \leq Z \leq 4$ were analysed in the frame of the Serber model modified to describe the two-step feature of the breakup reaction and to estimate absolute values of the formation cross sections for various isotopes. It was shown that the projectile breakup is the main mechanism responsible for the emission of intermediate mass clusters. The estimated cross sections for ^{10}He production are discussed in the context of its stability.

The investigation has been performed at the Laboratory of Nuclear Reactions, JINR.

Preprint of the Joint Institute for Nuclear Research. Dubna 1985